Inorganic Chemistry
Article

Inorg. Chem. **2009**, *48*, 7269–7279 **7269**
DOI: 10.1021/ic9006982

Sustained Water Oxidation by $[Mn_4O_4]^{7+}$ Core Complexes Inspired by Oxygenic Photosynthesis

Robin Brimblecombe,[†,‡] Derrick R. J. Kolling,[‡] Alan M. Bond,[†] G. Charles Dismukes,*[,‡,∥] Gerhard F. Swiegers,*[,§] and Leone Spiccia*[,†]

[†]*School of Chemistry, Monash University, Clayton, Victoria 3800, Australia,* [‡]*Department of Chemistry and the Princeton Environmental Institute, Princeton University, Princeton, New Jersey 08544, and* [§]*ARC Centre of Excellence for Electromaterials Science, Intelligent Polymer Research Institute, University of Wollongong, Wollongong, NSW 2522, Australia.* [∥]*New address: Department of Chemistry and Chemical Biology, Rutgers University, Busch Campus, Piscataway, New Jersey 08854.*

Received April 9, 2009

The bioinspired Mn-oxo cubane complex, $[Mn_4O_4L_6]^+$ **1b**$^+$ (L = (*p*-MeO-Ph)$_2$PO$_2$), is a model of the photosynthetic O_2-evolving complex. It is able to electro-oxidize water at 1.00 V (vs Ag/AgCl) under illumination by UV−visible light when suspended in a proton-conducting membrane (Nafion) coated onto a conducting electrode. Electrochemical measurements, and UV−visible, NMR, and EPR spectroscopies are interpreted to indicate that **1b**$^+$ is the dominant electro-active species in the Nafion, both before and after catalytic cycling, and thus correlates closely with activity. The observation of a possible intermediate and free phosphinate ligand within the Nafion suggests a catalytic mechanism involving photolytic disruption of a phosphinate ligand, followed by O_2 formation, and subsequent reassembly of the cubane structure. Several factors that influence catalytic turnover such as the applied potential, illumination wavelength, and energy have been examined in respect of attaining optimum catalytic activity. Catalytic turnover frequencies of 20−270 molecules O_2 h^{-1} catalyst^{-1} at an overpotential of 0.38 V plus light (275−750 nm) and turnovers numbers >1000 molecules O_2 catalyst^{-1} are observed. The **1b**$^+$-Nafion system is among the most active and durable molecular water oxidation catalysts known.

Introduction

Hydrogen (H_2) is a fuel that can be used to generate electricity in fuel cells with very high energy conversion efficiencies. It is, moreover, carbon free, generating only water as a byproduct when reacted with oxygen.[1] Efficient and economical processes for solar-powered generation of hydrogen from water are widely sought after as they potentially offer a sustainable and renewable fuel supply. Solar cells capable of water-splitting are electrochemical devices that combine a photoanode which oxidizes water (H_2O) into protons (H^+) and oxygen (O_2) (eq 1), coupled to a cathode where the protons are reduced to H_2 (eq 2).

$$\text{Photoanode}: 2H_2O \xrightarrow{h\nu} O_2 + 4H^+ + 4e \quad (1)$$

$$\text{Cathode}: 2H^+ + 2e^- \rightarrow H_2 \quad (2)$$

While water splitting can be achieved by electrolysis using noble metals, the process is energetically unfavorable, requiring an overpotential and thus cannot be easily driven by sunlight at ambient temperature. The most efficient electrocatalysts presently use Pt which has limited availability and requires an overpotential of 0.3 V at maximum current densities.[2] A range of challenges impede the utilization of semiconductors like TiO_2 and WO_3 as photocatalysts. These include wide bandgaps (3 eV), mismatches in the potential of the valence band edge and the water oxidation potential,[3−6] as well as physical instability under electrolysis conditions.[7,8] Another approach to developing water oxidation catalysts is to create, by electrodeposition, thermodynamically unstable phases of transition metal oxides that are catalytically active.[9] A recent example is the deposition of an amorphous

*To whom correspondence should be addressed. E-mail: dismukes@princeton.edu (G.C.D.), swiegers@uow.edu.au (G.F.S.), leone.spiccia@sci.monash.edu.au (L.S.).

(1) Turner, J. *Science* **2004**, *305*, 972–974.
(2) Anderson, A.; Neshev, N.; Sidik, R.; Shiller, P. *Electrochim. Acta* **2002**, *47*, 2999–3008.
(3) Miller, E. L.; Rocheleau, R. E.; Deng, X. M. *Int. J. Hydrogen Energy* **2003**, *28*, 615–623.
(4) Gratzel, M. *Nature* **2001**, *414*, 338–344.
(5) Yagi, M.; Tomita, E.; Sakita, S.; Kuwabara, T.; Nagai, K. *J. Phys. Chem. B* **2005**, *109*, 21489–21491.
(6) Nakamura, R.; Frei, H. *J. Am. Chem. Soc.* **2006**, *128*, 10668–10669.
(7) Arent, D. J.; Rubin, H. D.; Chen, Y. L.; Bocarsly, A. B. *J. Electrochem. Soc.* **1992**, *139*, 2705–2712.
(8) Rubin, H. D.; Arent, D. J.; Humphrey, B. D.; Bocarsly, A. B. *J. Electrochem. Soc.* **1987**, *134*, 93–101.
(9) Prasad, K. R.; Miura, N. *Electrochem. Commun.* **2004**, *6*, 1004–1008.

Published on Web 07/02/2009

Table 1. Catalytic Properties of Molecular Water Oxidation Catalysts Reported in the Literature[a]

complex	oxidant	support	TON	$K_{(O2)}$, h^{-1}
$([(bpy)_2Ru(OH_2)]_2O)^{4+}$ [11,12]	Ce^{4+}[b]	homogeneous	11−13	15
$[((tpy)_2(H_2O)Ru)_2(\mu\text{-dpp})]^{3+}$ [13]	Ce^{4+}[b]	homogeneous	19	50
$[Ru_2(macroN_6)(Rpy)_4Cl]^{3+}$ [16]	Ce^{4+}[b]	homogeneous	100−300	0.6
$[((Bu_2qui)(OH)Ru)_2(btpyan)]^{2+}$ [14]	1.9 V vs NHE, high pH	ITO	2400−33500	
$[(NH_3)_5Ru(\mu\text{-O})Ru(NH_3)_4(\mu\text{-O})Ru(NH_3)_5]^{6+}$ [15]	Ce^{4+}[b]	homogeneous		162
	1.6 V vs NHE	Nafion		11
$[Ru(NH_3)_4Cl_2]^{+}$ [15]	Ce^{4+}[b]	homogeneous		7.2
		Nafion		50
$[Ir(ppy)_2(H_2O)_2]^{+}$ [22]	Ce^{4+}[b]	homogeneous	2500	5.4
$[Mn_2(mcbpen)_2(H_2O)_2]^{2+}$ [20]	BuOOH[c]	homogeneous	13	1.5
$[((tpy)(H_2O)Mn)_2(\mu\text{-O})_2]^{3+}$ [18,31]	HSO_5^{-}[c] or ClO^{-}[c]	homogeneous	4	12
	Ce^{4+}[b]	Kaolin	17	
$[Mn_4O_4L_6]^{+}$ (**1b**$^{+}$)	1.2 V vs NHE	Nafion	> 1000[17]	20−270

[a] TON = number of catalytic turnovers; $K_{(O2)}$ = the turnover frequency. [b] Oxidative potential 1.7 V vs NHE. [c] Two electron oxygen donors.

non-conducting Co:P:O phase that catalytically facilitates water oxidation.[10]

A diverse range of non-biological, molecular water oxidation catalysts have been studied, including various ruthenium[11−16] and manganese complexes,[17−21] and a single class of iridium complexes.[22] A selection of these molecular catalysts, and the conditions under which they are active, are summarized in Table 1. As can be seen, the catalytic potential of these complexes has typically been investigated in homogeneous solution using chemical oxidants. This approach simplifies studies by eliminating the need for an electrochemical oxidation step. However, the chemical oxidants are, in many cases, directly implicated in, and active participants in the water oxidation reaction itself. Being non-innocent, these oxidants can complicate the interpretation of the intrinsic capabilities of the catalyst. By immobilizing the catalyst on an electrode surface, the oxidizing potential can be provided by direct electron transfer. This minimizes ambiguity regarding the origin of any evolved O_2 and provides a clearer indication of the practical utility of the catalysts in a water-oxidizing electrochemical device.

Nature has invented a single catalyst that sustains the photo-oxidation of water to oxygen. It is found in the *Photosystem II (PSII)* enzyme of all oxygenic phototrophs. *PSII* harbors an inorganic core, Mn_4CaO_x, denoted the *Water-Oxidizing Centre (WOC)*.[23,24] In the *PSII-WOC*, water is oxidized to O_2 and protons by a photoinduced reaction involving chlorophyll cation radical species ($P680^{+}$). The cation radical extracts 4 e^{-} from the *WOC* core in sequential photochemical steps at an average oxidation potential of 1.00 V vs Ag/AgCl.[25] P680 acts much like a hole generator/injector in a photovoltaic device.

The *PSII-WOC* has inspired a wide range of artificial model complexes.[26,27] The class of *PSII-WOC* mimics examined herein is the Mn-oxo cubanes, $[Mn_4O_4L_6]$ **1**, where $L^{-} = (p\text{-R-}C_6H_4)_2PO_2^{-}$; R = H (**1a**), OMe (**1b**) (Scheme 1).[27] The one-electron oxidized form of complex **1b**, denoted **1b**$^{+}$ (cubium) has previously been shown to catalyze, in a sustained way, the oxidation of water when doped into a proton conducting Nafion membrane immersed in an aqueous electrolyte.[17a] This catalytic activity was anticipated from the nearly stoichiometric evolution of O_2 from **1a**−**b** and **1a**$^{+}$-**1b**$^{+}$, following photodetachment of a phosphinate ligand upon UV photolysis in the gas phase.[28−30]

The cubanes fulfill several requirements for water oxidation catalysis. For example, they display a reaction pathway for the interconversion of water into O_2 at the catalytic core. A series of experiments have revealed that the cubane core readily exchanges and/or releases water, oxygen, and hydroxide molecules at corner oxo-positions (Scheme 1).[31] For example, **1a**−**b** can be oxidized to **1a**$^{+}$-**1b**$^{+}$ electrochemically or by using a strong acid and oxygen. The latter reaction occurs by protonation of an oxo followed by reduction by **1** (**1H**$^{+}$ + **1** → **1H** + **1**$^{+}$). The presence of the acid results in the release of a water molecule from **1H**, leaving the intermediate $Mn_4O_3L_6^{+}$, which subsequently reacts with O_2 in air to form **1**$^{+}$ in nearly stoichiometric yield.

Another prerequisite for efficient water oxidation catalysis is cooperative multielectron redox chemistry. The cubanes display this attribute in several reactions. For example,

(10) Kanan, M. W.; Nocera, D. G. *Science* **2008**, *321*, 1072–1076.
(11) Binstead, R. A.; Chronister, C. W.; Ni, J.; Hartshorn, C. M.; Meyer, T. J. *J. Am. Chem. Soc.* **2000**, *122*, 8464–8473.
(12) Collin, J. P.; Sauvage, J. P. *Inorg. Chem.* **1986**, 25.
(13) Sens, C.; Romero, I.; Rodriguez, M.; Llobet, A.; Parela, T.; Benet-Buchholz, J. *J. Am. Chem. Soc.* **2004**, *126*, 7798–7799.
(14) Tohru Wada, K. T. K. T. *Angew. Chem., Int.Ed.* **2000**, *39*, 1479–1482.
(15) Yagi, M.; Kentaro Nagoshi, M. K. *J. Phys. Chem. B* **1997**, *101*, 5143–5146.
(16) Zong, R.; Thummel, R. P. *J. Am. Chem. Soc.* **2005**, *127*, 12802–12803.
(17) (a) Brimblecombe, R.; Swiegers, G. F.; Dismukes, G. C.; Spiccia, L. *Angew. Chem., Int. Ed.* **2008**, *120*, 7445–7448. (b) Brimblecombe, R.; Bond, A. M.; Dismukes, G. C.; Swiegers, G. F.; Spiccia, L. *Phys. Chem. Chem. Phys.* **2009**, DOI: 10.1039/ B901419E.
(18) Limburg, J.; Vrettos, J. S.; Liable-Sands, L. M.; Rheingold, A. L.; Crabtree, R. H.; Brudvig, G. W. *Science* **1999**, *283*, 1524–1527.
(19) Kurz, P.; Berggren, G.; Anderlund, M. F.; Styring, S. *Dalton Trans.* **2007**, 4258–4261.
(20) Poulsen, A. K.; Rompel, A.; McKenzie, C. J. *Angew. Chem., Int.Ed.* **2005**, *44*, 6916–6920.
(21) Shimazaki, Y.; Nagano, T.; Takesue, H.; Ye, B.-H.; Tani, F.; Naruta, Y. *Angew. Chem., Int. Ed.* **2004**, *43*, 98–100.
(22) McDaniel, N. D.; Coughlin, F. J.; Tinker, L. L.; Bernhard, S. *J. Am. Chem. Soc.* **2008**, *130*, 210–217.
(23) Dasgupta, J.; vanWilligen, R. T.; Dismukes, G. C. *Phys. Chem. Chem. Phys.* **2004**, *6*, 4793–4802.
(24) Messinger, J. *Phys. Chem. Chem. Phys.* **2004**, *6*, 4764–4771.
(25) Rappaport, F.; Guergova-Kuras, M.; Nixon, P. J.; Diner, B. A.; Lavergne, J. *Biochem.* **2002**, *41*, 8518–8527.
(26) Cady, C. W.; Crabtree, R. H.; Brudvig, G. W. *Coord. Chem. Rev.* **2008**, *252*, 444–455.
(27) Ruettinger, W.; Dismukes, G. C. *Chem. Rev.* **1997**, *97*, 1–24.
(28) Ruettinger, W. F.; Dismukes, G. C. *Inorg. Chem.* **2000**, *39*, 1021–1027.
(29) Yagi, M.; Wolf, K. V.; Baesjou, P. J.; Bernasek, S. L.; Dismukes, G. C. *Angew. Chem., Int. Ed.* **2001**, *40*, 2925–2928.
(30) Wu, J.-Z.; Angelis, F. D.; Carrell, T. G.; Yap, G. P. A.; Sheats, J.; Car, R.; Dismukes, G. C. *Inorg. Chem.* **2006**, *45*, 189–195.

Scheme 1. (**top images**) Perfluorinated Polymer Backbone of Nafion (left) Forms a Hydrophobic Solid Membrane (right) That Is Penetrated by Aqueous Channels Lined with Hydrophilic, Ionizable, Sulfonic Acid Groups, $-SO_3H$[a]; (**bottom images**) Previously Characterized Cubane Reactions (Solid Arrows) for $[Mn_4O_4L_6]$ (**1**)[b], and a Proposed Catalytic Photo-Electrolysis Reactions (Dashed Arrows) Showing Light-Driven and Electrode-Driven Processes Predicted from This Work[c]

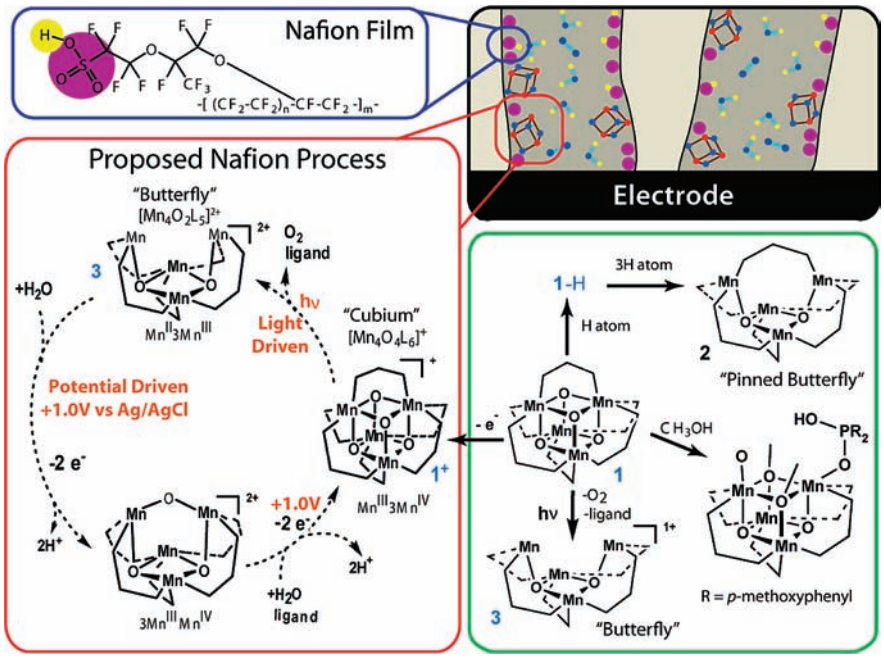

[a] Cubes represent the intact precursor catalyst molecules $[Mn_4O_4((CH_3OPh)_2PO_2)_6]^+$ (**1b**$^+$) which are taken into the sulfonate-lined aqueous channels by ion exchange, displacing protons and remaining loosely associated with sulfonate anions. [b] **RHS**. [c] **LHS**; for the two proposed intermediates ($Mn^{II}3Mn^{III}$ and $3Mn^{III}Mn^{IV}$). Ligated water completing the manganese coordination sphere have been omitted for clarity.

1a$^+$ oxidizes organic amines via two-electron/one-proton (hydride) abstraction, without participation of one-electron redox intermediates,[32] while **1a** catalyzes oxo transfer to organic thioethers forming sulfoxides and sulfones.[54]

In a previous communication,[17a] we described a method for inducing the cubanes to undertake catalytic water oxidation by transfer into Nafion, a proton-conducting electrolyte membrane. Nafion is a hydrophobic, fluorinated polymer with highly acidic sulfonic acid head groups (Scheme 1: top image).[33] These hydrophilic head groups form interconnected aqueous channels occupied by mobile cations (H^+ or Na^+) within the hydrophobic polymer domain (diameters ca. 20−30 nm).[33] These channels are permeable to various cations but not anions as they are lined with the sulfonate anions.[34] Nafion is widely used as a proton exchange membrane[33,35] and has been used to support a range of metal based catalysts,[33] including water oxidation catalysts whose performance was improved by doping into Nafion (Table 1 gives some examples).[15]

Herein, we examine the nature of the light-assisted electrooxidation of water by **1b**$^+$ in Nafion/electrode assemblies using UV−visible, NMR, and electron paramagnetic resonance (EPR) spectroscopies, as well as cyclic voltammetry. We establish the presence of intact $[Mn_4O_4L_6]^+$ within the Nafion membrane before and after catalysis and that a previously unobserved manganese complex is formed during the catalytic cycle. We report further catalytic turnover data revealing that **1b**$^+$-Nafion is, or is a precursor to, one of the most active and stable molecular water oxidation catalysts reported to date.

Experimental Section

Materials and Methods. Compounds **1b**[36] and **1b**$^+$ ClO_4^- [30] were prepared as described previously. **1b**$^+$ $CH_3C_6H_4SO_3^-$ was prepared as per **1b**$^+ClO_4^-$ [30] with $CH_3C_6H_4SO_3H$ used in place of perchloric acid. Diphenylphosphinic acid and bis(methoxyphenyl)phosphinic acid were purchased from Lancaster and Aldrich, respectively, and used without further purification. Tetrabutylammonium hexafluorophosphate (Bu_4NPF_6) was obtained from GFS Chemicals and used as the electrolyte in organic solvents after purification.[17] Nafion was purchased from DuPont and Sigma as acidic polymer dispersions, DE 1020, 10−12% aqueous dispersion, and 117 Nafion, 5% solution in alcohol, respectively. All other reagents were purchased from BDH or Aldrich. The pH of the aqueous solutions and buffers used in electrochemical studies were adjusted to pH 3.3 and 7, by titration with either 0.1 M H_2SO_4 or 0.1 M NaOH, in the presence of Na_2SO_4 supporting electrolyte (ionic strength 0.1 M).

Electrochemistry. Electrochemical experiments were conducted at 22(±2) °C with BAS (Bio Analytical Systems) Epsilon CS3 or 100B workstations. Cyclic voltammograms were obtained at scan rates of 5 to 500 mV s^{-1} in a conventional electrochemical cell containing a three-electrode system. Experiments in CH_3CN (0.1 M Bu_4NPF_6), used a Ag/Ag^+ reference

(31) Narita, K.; Kuwabara, T.; Sone, K.; Shimizu, K. i.; Yagi, M. *J. Phys. Chem. B* **2006**, *110*, 23107–23114.
(32) Carrell, T. G.; Bourles, E.; Lin, M.; Dismukes, G. C. *Inorg. Chem.* **2003**, *42*, 2849–2858.
(33) Seen, A. J. *J. Mol. Catal. A: Chem.* **2001**, *177*, 105–112.
(34) Gargas, D. J.; Bussian, D. A.; Burratto, S. K. *Nano Lett.* **2005**, *5*, 2184.
(35) Hoyer, B.; Jensen, N.; Busch, L. P. *Electroanalysis* **2001**, *13*, 843–848.
(36) Ruettinger, W. F.; Campana, C.; Dismukes, G. C. *J. Am. Chem. Soc.* **1997**, *119*, 6670–6671.

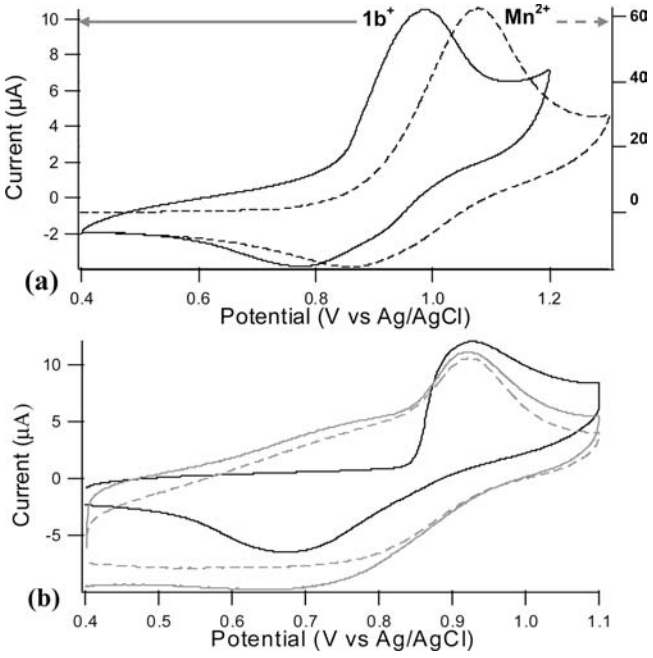

Figure 1. Cyclic voltammograms obtained at 22 °C in aqueous 0.1 M Na_2SO_4, scan rate: 50 mV s^{-1}: (a) $\mathbf{1b}^+$/Nafion-glassy carbon (black solid line) current scale on left and $\mathbf{Mn}^{2+}$/Nafion-glassy carbon (black dashed line) displaying current scale on right, electrodes. (b) $\mathbf{1b}^+$/Nafion-glassy carbon before illumination with light (black solid line), after 1 h poised at 1.00 V (vs Ag/AgCl) with illumination by light (gray solid line) and after 2 h (gray dashed line).

(0.01 M $AgNO_3$ in acetonitrile) prepared and calibrated as described elsewhere.[17] Aqueous experiments were conducted in distilled water containing 0.1 M Na_2SO_4 as the electrolyte. In this case, potentials were referenced against a BAS Ag/AgCl (3 M NaCl) glass bodied reference electrode, with a potential of 0.200 V vs NHE at 25 °C (BAS reference electrode users manual). Potentials are reported relative to this reference electrode unless otherwise stated. All experiments used Pt wire or mesh auxiliary electrodes.

As shown in Figure 1a, the cyclic voltammetry of $\mathbf{1b}^+$ when supported in Nafion was typically commenced at 1 V, and initially sweeping to more negative values of about 0.4 V to reduce $\mathbf{1b}^+$ plus to **1** (this sweep not shown for clarity) and then cycling over the range of 0.4 to 1.0 V. On some occasions, such as in Figure 1b, the potential was held at 0.4 V prior to commencement of cycling.

The range of working electrodes studied included glassy carbon (GC), Pt disk, Pt plate, and fluorine tin oxide (FTO) conductive glass. The glassy carbon working electrode had a diameter of 3 mm (electroactive area of 5.9 mm^2, as determined by oxidation of 1.0 mM ferrocene in CH_3CN (0.5 M Bu_4NPF_6) and use of the Randles−Sevcik equation[37] with a diffusion coefficient (D) of 1.7×10^{-5} /cm^2 s^1).

Nafion Film Deposition and Doping. Nafion-modified electrodes were prepared by drop casting 2%, 5%, or 10% Nafion suspensions onto the working electrode, air drying and then heating in an oven at 120 °C for 20 min. Doping of the Nafion membrane was achieved by immersion of the Nafion- coated electrode in 2 mM solutions of $\mathbf{1b}^+$ ClO_4^-, $\mathbf{1b}^+$ $CH_3C_6H_4SO_3^-$ or $[Mn(OH_2)_6]$ $(ClO_4)_2$.

Photoelectrochemical Measurements. Light excitation and cyclic voltammetry experiments were conducted in a glass cell using either a glassy carbon, Pt, or FTO working electrode (photoanode, water oxidation) with a Pt wire counter electrode (cathode) and either the aqueous (Ag/AgCl) or the organic (Ag/Ag^+) reference electrode.

Light Source. The xenon light source used for these experiments generated white light with a stable output over the range 250−750 nm, from a Rofin Australia-Polilight PL6, passed through a 1 m long liquid light guide. A silicon diode calibrated against a Solar Simulator (1000 W Xe, Oriel) was used to determine the light intensity for individual experiments (typically at 150 mWm^{-2}). A 365 nm Nichia-LED, with λ bandwidth $\pm$ 5 nm and output power of 5 mW/cm^2, was placed approximately 2 cm from the electrode, with light passing through 3 mm of glass before reaching the sample.

UV−visible Spectrophotometry. UV−visible spectra of $\mathbf{1b}^+$, in CH_2Cl_2 or Nafion, were recorded in 1 cm quartz cuvettes using a Varian Cary 300 BIO-spectrometer. Nafion membranes were prepared and doped on the inside of quartz cuvettes. As the $\mathbf{1b}^+$ concentration in Nafion support was not known, molar extinction coefficients were not calculated from the absorbance data.

NMR. NMR spectra were measured at 25 °C on a Varian Mercury-Vx 300-MHz Spectrometer using quartz tubes. Solutions of $\mathbf{1b}^+$ ClO_4, sodium bis(*p*-methoxyphenyl)phosphinate or $CH_3C_6H_4SO_3^-$ were analyzed in deuterated acetone. Membranes were cast on the inside of quartz NMR tubes, dried, doped, and rinsed with CH_3CN. Nafion samples were solvated with deuterium oxide (D_2O).

EPR. EPR spectra were recorded using a Bruker Elexsys 580 X-band spectrometer and Bruker ER 4116DM dual-mode EPR cavity. The measurements were made at a temperature of 5 K using an Oxford ESR 900 helium flow cryostat, at a microwave frequency of 9.63 GHz, with microwave power of 20 mW and modulation amplitude of 1 mT. Samples were prepared by casting Nafion membranes onto ITO glass, which were then cut from the glass using a razor blade and transferred to EPR tubes.

Results and Discussion

Doping of Nafion. In a typical experiment, a 3 mm diameter glassy carbon electrode was coated with a thin layer of Nafion and dried. SEM analysis indicated that each Nafion layer was quite uniform (Supporting Information, Figure S1) and that the thickness could be systematically varied between 3 and 8 μm depending on the concentration of the Nafion suspension used. Doping of the electrode-Nafion assembly was achieved by immersing it in a 2 mM acetonitrile solution of $\mathbf{1b}^+$. Subsequent washing and immersion of the doped electrode in an aqueous solution (0.1 M Na_2SO_4) exchanged the solvent and trapped the water- insoluble $\mathbf{1b}^+$ cations in the Nafion layer (Scheme 1: top right). Cyclic voltammetry of the doped Nafion electrode immersed in aqueous electrolyte indicated a redox process at a similar potential to that previously observed for the $\mathbf{1b}/\mathbf{1b}^+$ couple (Figure 1a).[17b] This couple was not present in undoped Nafion (Supporting Information, Figure S2). Oxidation of **1b** to $\mathbf{1b}^+$ in the doped Nafion was achieved at 1.00 V, the potential used for photolysis.

Photo-Electrochemical Experiments. Details of the device assembly used for these measurements were provided in our communication.[17a] Briefly, photoanodes, constructed as detailed in the Experimental Section, were assembled into working devices by combining them with a Pt counter electrode (cathode) and an electrolyte solution (typically an aqueous solution containing 0.1 M Na_2SO_4). A transient current was observed from $\mathbf{1b}^+$-Nafion electrodes upon first application of a 1.00 V bias.

(37) Bard, A. J.; Faulkner, L. R. *Electrochemical Methods: Fundamentals and Applications*; John Wiley & Sons, Inc.: New York, 1990.

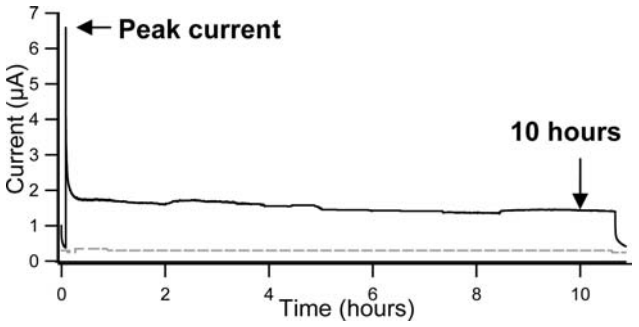

Figure 2. Time dependence of the photocurrent detected at a 3 mm diameter glassy carbon electrode at a potential of 1.00 V vs Ag/AgCl, for **1b**$^+$-Nafion/glassy-C (black) and undoped-Nafion/glassy-C (gray) photoanodes in contact with aqueous 0.1 M Na_2SO_4. Illumination by a white light source starts at 10 min; light source switched off after 10 h.

Following decay of this current, essentially to zero, a significant photocurrent is observed when illuminated with light (275−750 nm; Figure 2). This photocurrent was found to continue over at least 65 h of testing.[17a] It commences immediately upon illumination and disappears when the light source is turned off.

The net photocurrent in such experiments (Figure 2), which is the photocurrent with the background current subtracted, is typically more than 20× that observed for an equivalent electrode in which the Nafion layer is not doped with **1b**$^+$. The magnitude and persistence of the photocurrent over such extended periods of time indicates that the system does not obtain its electrons from sacrificial decomposition of **1b**$^+$. The fact that undoped Nafion-coated electrodes did not yield a significant photocurrent indicates that the Nafion does not provide the electrons. The only potential alternatives as electron sources are the water and the Na_2SO_4 in the aqueous solution. The latter is unlikely given that SO_4^{2-} is in a highly oxidized state and testing of these electrodes in a range of electrolytes (NaF, Bu_4NPF_6, Bu_4NClO_4) yielded equivalent photocurrents.[17a] Moreover, the photocurrent was observed for **1b**$^+$-doped Nafion membranes deposited on a range of conductive surfaces (glassy carbon, Pt, and F-doped SnO_2 coated glass). No photocurrent was observed for Nafion-electrodes doped with salts like $NaClO_4$ or sodium bis(methoxyphenyl)phosphinate (counteranion and ligand, respectively). The only remaining electron source was therefore the bulk water in the electrolyte solution.

To test the hypothesis that water is the source of electrons for photocurrent generation, the **1b**$^+$-Nafion-coated electrodes were tested in acetonitrile solution (0.1 M Bu_4NPF_6), into which were titrated increasing quantities of water (Figure 3). The photocurrent was essentially zero in pure acetonitrile and increased in proportion to the amount of water added, up to 8% (v/v) H_2O/CH_3CN. Thereafter, the photocurrent saturated, with no further change with increasing water content.

As noted in eq 1, water oxidation is accompanied by the generation of protons, as shown in our communication.[17a] The photocurrent was found to increase linearly with solution pH between 2 and 12, as expected for a water oxidation process in which protons were generated. These changes were accompanied by a net production of O_2 gas, whose quantity corresponded closely to that expected

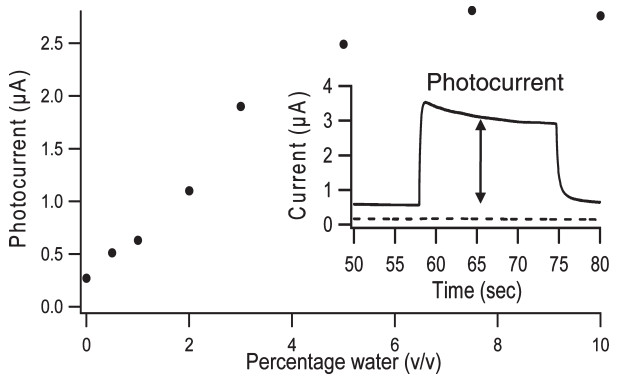

Figure 3. Photocurrent from a **1b**$^+$-Nafion/glassy carbon electrode poised at 1.00 V (vs Ag/AgCl) as a function of increasing water content (% v/v), in acetonitrile (0.1 M Bu_4NPF_6). Inset displays controlled potential photocurrent at 1.00 V, for **1b**$^+$-Nafion/glassy carbon electrode in acetonitrile containing 10% (v/v) water (solid line) and 0% water (dashed line). Photocurrent shown by arrow.

from the cumulative charge passing through the electrode. Additionally, when the system was immersed in ^{18}O-water (50% $H_2{}^{18}O$, 0.1 M Na_2SO_4), a significant increase in $^{18}O_2$ concentration (m/z = 36) was observed.[17a] Thus, bulk water is unquestionably the source of electrons responsible for the photocurrent and O_2 is the product at the anode.

Role of the Applied Potential. A linear sweep voltammogram of an undoped Nafion-coated glassy carbon electrode revealed no significant currents negative of about 1.25−1.30 V (vs Ag/AgCl) (Supporting Information, Figure S2). When the Nafion coating is doped with **1b**$^+$, a new redox process appeared at 0.80−1.00 V (Figure 1a), corresponding to the **1b/1b**$^+$ oxidation process. Positive of these potentials, an increasing current due to water oxidation is observed. The couple was quite different to the comparable $Mn^{II/IV}$ oxidation process observed for membranes doped with Mn^{2+} (Figure 1a; Mn^{2+} trace).[17b]

To establish the influence of the applied potential on photocurrent, we measured the photocurrent under constant illumination at various applied potentials. The net photocurrent (background dark current subtracted) increases from near zero at potentials negative of 0.80 V to reach a maximum at about 1.00 V. At potentials positive of 1.00 V, it remains constant up to 1.20 V (Figure 4b). This maximum at 1.00 V corresponds to the complete oxidation of the species responsible for the catalytic photocurrent. The photocurrent reached its peak value at the same potential as the complete oxidation of **1b** to **1b**$^+$ in the dark, as seen in linear sweep voltammetry (Figure 4c). This suggests that the role of the applied potential is only to generate **1b**$^+$ or a closely related catalytically active species. Increasing the potential further increased the overall current, but did not increase the photocurrent, suggesting the catalyzed oxidation of water occurs in two steps, an electrode driven step and a light driven step (Scheme 1 (Nafion Process)).

Cyclic voltammetry of **1b**$^+$-Nafion/glassy carbon recorded (in the dark) after catalytic cycling by illumination at 1.00 V in water for 2 h, revealed that the **1b/1b**$^+$ couple was still observed at the same potential and with peak currents similar to those seen before catalytic cycling

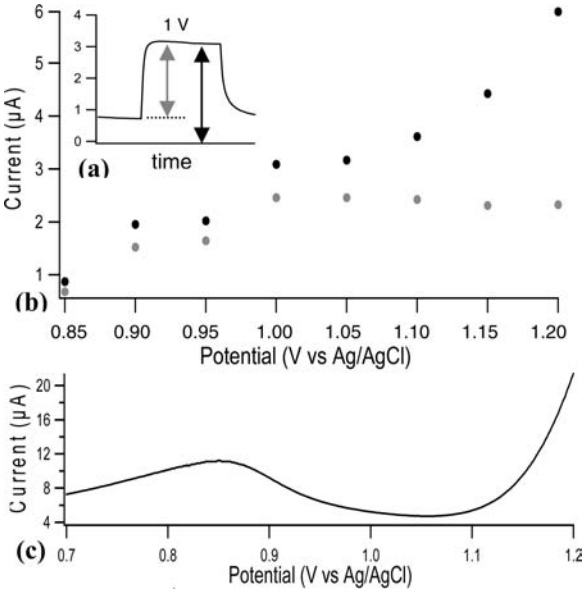

Figure 4. $\mathbf{1b}^+$/Nafion-glassy carbon electrode in aqueous (0.1 M Na_2SO_4): (a) Controlled potential photocurrent at 1.00 V (vs Ag/AgCl) illuminated (275−750 nm), black arrow defining total current = dark + photocurrent, gray arrow defining photocurrent only = total current − dark current. (b) Total current (black dots), and photocurrent (gray dots) plotted against individual potential steps of 0.05 V. (c) Linear sweep voltammetry of **1b** to $\mathbf{1b}^+$ at 50 mVs^{-1} in the dark, **1b** initially formed by the reduction of $\mathbf{1b}^+$ at 0.7 V.

(Figure 1b). Thus, nearly all of the cubane remained present and electroactive within the Nafion. After catalytic cycling for 2 h, in addition to the $\mathbf{1b/1b}^+$ couple, there was an increase in the underlying current indicative of a change in the capacitance of the cell. This change was associated with the appearance of a very broad peak for an oxidation process at less positive potentials (0.70 V), indicating the formation of a new (minor) species. The emergence of this peak is suggestive of either an intermediate species in the catalytic process or a side-product.

Cyclic voltammetry of $\mathbf{1b}^+$ in CH_2Cl_2 (0.1 M Bu_4NPF_6) under conditions of ambient illumination indicated that there were no redox processes between 0.80 and 2.00 V, the solvent limit. For undoped Nafion-GC electrodes in aqueous electrolyte, a substantial dark current was observed positive of about 1.40 V (Supporting Information, Figure S2), which is due to water oxidation. In the absence of illumination, the current due to water oxidation was enhanced by the $\mathbf{1b}^+$-doped Nafion coating at potentials positive of 1.20 V (Supporting Information, Figure S2). These observations reveal that a limited rate of water oxidation catalysis was achieved by the cubane in darkness at these higher potentials.

EPR Spectra. The EPR spectrum of a $\mathbf{1b}^+$-Nafion membrane revealed a distinctive signal with four peaks below 2500 G indicative of oxidized cubanes, based on its known EPR signal in non-aqueous solution (Figure 5).[28] The neutral parent cubane, **1b**, is diamagnetic and EPR silent.

Controlled potential electrolysis of $\mathbf{1b}^+$-Nafion membranes followed by measurement of the EPR spectrum revealed that when poised at potentials more negative than 0.60 V, the $\mathbf{1b}^+$ EPR signal decreased, consistent

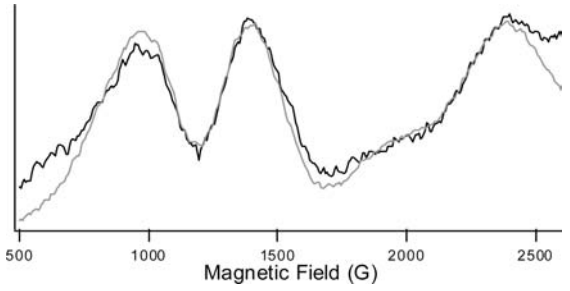

Figure 5. Low field region of the EPR spectrum of $\mathbf{1b}^+$ in Nafion after polarization at 1.00 V (vs Ag/AgCl) in aqueous 0.1 M Na_2SO_4 (gray solid line), and of pure $\mathbf{1b}^+$ dissolved in CH_2Cl_2 (black solid line). Measurement parameters are listed in the Experimental Section.

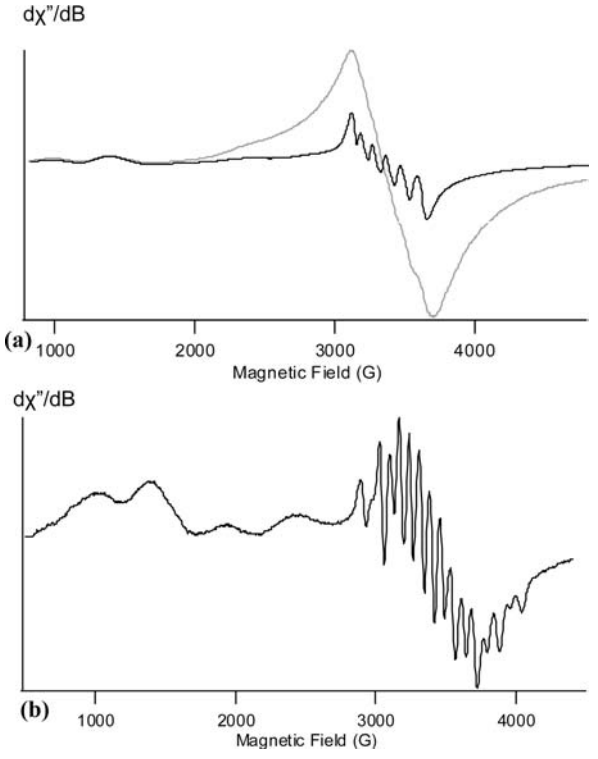

Figure 6. EPR spectrum of $\mathbf{1b}^+$: (a) In unbiased Nafion (gray solid line) and dissolved in CH_2Cl_2 (black solid line), displaying cubane features to the left and Mn^{2+} features to the right. (b) In Nafion after polarization at 1.00 V (vs Ag/AgCl) in aqueous 0.1 M Na_2SO_4, displaying cubane features on the left and features characteristic of an oxo-bridged Mn^{III}-Mn^{IV} species on the right. Measurement parameters are listed in the Experimental Section.

with the formation of an EPR silent form. When poised at +1.00 V, the signal corresponding to $\mathbf{1b}^+$ increased. Thus, EPR spectroscopy supports the proposal that the redox process in the cyclic voltammogram in Figure 1 corresponds to the previously reported $\mathbf{1b} \leftrightarrow \mathbf{1b}^+ + e^-$ process.[38]

In addition to the $\mathbf{1b}^+$ EPR signal, a signal characteristic of the presence of Mn^{2+} ions was observed in Nafion following doping and prior to electrochemical biasing (Figure 6a). This signal appears in a different spectral window ($g = 2$) and was also observed in the acetonitrile doping solution containing $\mathbf{1b}^+$. The signal is believed

(38) Wu, J.-Z.; Sellitto, E.; Yap, G. P. A.; Sheats, J.; Dismukes, G. C. *Inorg. Chem.* **2004**, *43*, 5795–5797.

to arise from an impurity introduced during cubane synthesis and/or a degradation product of the oxidized cubane.

The intensity of the EPR signal of Mn^{2+} relative to $\mathbf{1b}^+$ was higher for the Nafion film relative to $\mathbf{1b}^+$ in the doping solution. This was expected since dications are preferentially exchanged into the anionic-Nafion during the doping process, when compared to the bulky singly charged cubium cluster, $\mathbf{1b}^+$.

The EPR signal of Mn^{2+} is considerably more intense than the signal from an equal amount of $\mathbf{1b}^+$. The concentration ratio of Mn^{2+} to $\mathbf{1b}^+$ in the Nafion was estimated by comparison of the integral areas of the two EPR signals following isolation of each spectrum by subtraction of the spectrum of pure $\mathbf{1b}^+$ (Figures 5 and 6a).[39] The relative spin concentrations were estimated from the product of the signal areas and the EPR transition probability, as described in the Supporting Information, Figure S4. These data indicate that the Mn^{2+} concentration in Nafion is between 1.6% and 5% that of $\mathbf{1b}^+$.

Cyclic voltammetry of the $\mathbf{1b}^+$/Nafion membranes reveal no detectable Mn^{II}/Mn^{IV} couple (Figure 1a), indicating that the Mn^{2+} observed by EPR spectroscopy is a very small fraction of the electroactive species present in the membrane.

Examination of the EPR spectrum of $\mathbf{1b}^+$-Nafion after extended polarization at 1.00 V under both illumination and non-illumination conditions (Figure 6b) revealed that $\mathbf{1b}^+$ remained the dominant species in Nafion. The minority Mn^{II} signal with its characteristic hyperfine splitting was almost completely lost upon electrode polarization. We propose that the Mn^{2+} species was converted into an EPR-silent species, consistent with the expected formation of solid MnO_2, which has a very broad and weak EPR signal.

To further investigate the possible role of Mn^{2+} in the electrochemical response, Nafion-coated electrodes were doped with Mn^{2+} from an acetonitrile solution of $[Mn(OH_2)_6](ClO_4)_2$ (2 mM in 50 mM $HClO_4$). Cyclic voltammetry (see Figure 1a) shows that the Nafion membranes doped with Mn^{2+} display larger oxidation peak currents in the dark, of about 60 μA, compared to peak currents of about 10 μA for $\mathbf{1b}^+$ doped membranes. This was consistent with the more efficient uptake of Mn^{2+} ions into Nafion. However, only a small photocurrent was observed; this was about one-seventh of that observed for the less concentrated $\mathbf{1b}^+$-Nafion system (Supporting Information, Figure S3). As discussed above, the contaminating Mn^{2+} is not electrochemically detected in $\mathbf{1b}^+$-doped membranes (Figure 1a). Thus, the contribution to the photocurrent by the Mn^{2+} in $\mathbf{1b}^+$-doped membranes is estimated to be insignificant. The observation of a small photocurrent from Mn^{2+}/Nafion electrodes was in contrast to our earlier work where no significant photocurrent was seen from Mn^{2+} doped Nafion membranes.[17a] The present experiments differ from our previous study in the use of dilute concentrations of a strong acid ($HClO_4$) in the doping process, which we now know to be important for effective penetration of ions into Nafion.

After extended polarization of $\mathbf{1b}^+$-Nafion at 1.00 V (> 10 min) with and without illumination, a 16-line EPR spectrum was observed (only at low temperature, ca. 5 K) in addition to the intact $\mathbf{1b}^+$ cubium EPR signal (Figure 6b). As a class, these types of multiline EPR signals have been widely studied and are customarily associated with μ-oxo-bridged (both mono- or di-μ-oxos) complexes containing a spin-coupled $Mn^{III}Mn^{IV}$ unit, either alone or embedded within a larger diamagnetic cluster.[40−43] Continued illumination of these samples in the absence of applied bias resulted in a decrease in the 16-line signal and an increase in the 6-line Mn^{2+} signal. The 16-line EPR signal is not observed for solutions of **1b** or $\mathbf{1b}^+$ dissolved in acetonitrile and electrically unbiased $\mathbf{1b}^+$/Nafion membranes both before and after irradiation, nor for Mn^{2+}-doped Nafion electrically biased under equivalent conditions.

Analysis of the spectrum reveals it to be different from the EPR spectrum of the $[Mn_2O_2(bipy)_4]^{2+}$ precursor used for cubane synthesis. EPR, UV−vis, and NMR spectroscopies provided no evidence for $[Mn_2O_2(bipy)_4]^{2+}$ contamination in any of the cubane samples. Further, as expected, the EPR spectra of authentic $[Mn_2O_2(bipy)_4]^{3+}$ in Nafion after polarization at 1.00 V revealed this electrolysis product to be EPR silent ($2Mn^{IV}$). Consequently, the 16-line species in Figure 6b is proposed to be a product of an electrolytic reaction of the $\mathbf{1b}/\mathbf{1b}^+$ cubium within hydrated Nafion.

We speculate that the species responsible for the 16-line spectrum may be the origin of the new oxidation process observed by cyclic voltammetry after extended catalytic cycling (Figure 1b). As described herein and previously,[17] the reaction between $\mathbf{1b}^+$ and water in aqueous Nafion forms a reduced intermediate (slow in the dark and fast under light) that can be reoxidized electrochemically to reform $\mathbf{1b}^+$. Although the evidence for the identity of this intermediate is inconclusive, it suggests the formation of a butterfly like species related to $[L_5Mn_4O_2]^{2+}$, which is observed following O_2 release in the gas phase reaction.[44] Oxidation of this reduced species ($Mn^{II}3Mn^{III}$) is a reasonable starting point for the formation of the species with the 16-line EPR spectrum by electrolysis (Scheme 1, bottom RHS).

A 16-line EPR signal has never been seen before from any of the Mn-oxo cubane systems we have worked with and is, consequently, a new species to identify. The ^{55}Mn hyperfine interaction, which is responsible for the 16-line structure, provides a direct measure of the unpaired electron spin density residing on Mn ions (scalar part only) and so is useful in describing the degree of spin density transferred onto neighboring ligands through covalency.[40] The overall spectral breadth of the ^{55}Mn hyperfine field of the 16-line species is 105.2 mT (outermost

(39) Ruettinger, W. F.; Ho, D. M.; Dismukes, G. C. *Inorg. Chem.* **1999**, *38*, 1036–1037.

(40) Cooper, S. R.; Dismukes, G. C.; Klein, M. P.; Calvin, M. *J. Am. Chem. Soc.* **1978**, *100*, 7248–7252.

(41) Schafer, K. O.; Bittl, R.; Lendzian, F.; Barynin, V.; Weyhermuller, T.; Wieghardt, K.; Lubitz, W. *J. Phys. Chem. B* **2003**, *107*, 1242–1250.

(42) Schafer, K. O.; Bittl, R.; Zweygart, W.; Lendzian, F.; Haselhorst, G.; Weyhermuller, T.; Wieghardt, K.; Lubitz, W. *J. Am. Chem. Soc.* **1998**, *120*, 13104–13120.

(43) Zheng, M.; Khangulov, S. V.; Dismukes, G. C.; Barynin, V. V. *Inorg. Chem.* **1994**, *33*, 382–387.

(44) Ruettinger, W.; Yagi, M.; Wolf, K.; Bernasek, S.; Dismukes, G. C. *J. Am. Chem. Soc.* **2000**, *122*, 10353–10357.

peak-to-peak range). For the purpose of quantitative analysis, this is equal to the sum $5A_1+5A_2+5a^{\text{dipolar}}$ where A_i are the scalar hyperfine coupling constants of the two Mn ions and a^{dipolar} is the dipolar part of the hyperfine interactions from both Mn^{III} and Mn^{IV}.[40,43] The value of a^{dipolar} is 15−25% of the scalar hyperfine field ($5A_1+5A_2$) for all dimanganese(III,IV) examples that we are familiar with.[41−43] This suggests an upper limit for the scalar hyperfine field of 101.0 mT for the 16-line intermediate.

We have compared this total scalar hyperfine field to that reported for 10 structurally characterized examples of di-μ-oxo-dimanganese(III,IV) complexes in which both Mn ions have either N_3O_3 or N_4O_2 hexacoordinate ligand fields, as well as to the Mn catalase enzyme from *Thermus thermophilus* also in the (III,IV) oxidation state and which has Mn ions with N_1O_5 hexacoordinate ligand fields and a di-μ-oxo bridge.[41−43,45] In this series of 11 complexes, the value of $5A_1+5A_2$ ranges between 106.5 mT to 121.0 mT with a mean value of 112.8 mT. This comparison reveals that the 16-line intermediate exhibits a significantly smaller scalar hyperfine field than all 11 reference examples (10% smaller that the mean value) and reflects a substantially reduced spin density on Mn ions compared to these reference compounds. The 16-line intermediate exhibits appreciably greater transfer of spin density onto the coordinated ligands and/or oxo bridges than the reference set.

Although the chemical composition of this species is unknown, this analysis of the 16-line EPR signal strongly suggests that it is composed of a Mn_x cluster with a low-spin ($S = 1/2$) ground state and containing, at minimum, a spin-coupled $Mn^{III}Mn^{IV}$ center, possessing unusually low spin density on the Mn ions. However, the presence of other more strongly spin-coupled Mn ions within this cluster (e.g., diamagnetic subcluster contributing no spin density to the ground state)[41−43] cannot be excluded. Consequently, a spin-coupled tetramanganese cluster with a weakly coupled $Mn^{III}Mn^{IV}$ subcluster is also a potential candidate. At this stage it is unclear whether this species is a catalytic intermediate or involved in a terminal side reaction, although we have suggested the former (Scheme 1).

UV−visible Spectra. Figure 7 depicts the UV−visible absorption spectrum of **1b**$^+$, both as a free species in CH_2Cl_2 and as a dopant in electrically unbiased Nafion (cast and doped on the inside of a quartz cuvette and then placed in contact with water). Free **1b**$^+$ in dichloromethane displays several substantial absorption bands in the UV/visible region, with a maximum at about 220 nm. Absorption at this wavelength is primarily due to the phenyl rings of the phosphinate ligands.

When **1b**$^+$ was ion-exchanged into Nafion from acetonitrile, an absorption band was observed at 250 nm, which was 30 nm red-shifted from that in CH_2Cl_2 (Figure 7). Equivalent spectra were observed for **1b**$^+$/Nafion membranes in dry air or immersed in water. Casting of the neutral diphenylphosphinic acid into Nafion revealed an equivalent red shift relative to solution spectra. Thus, the

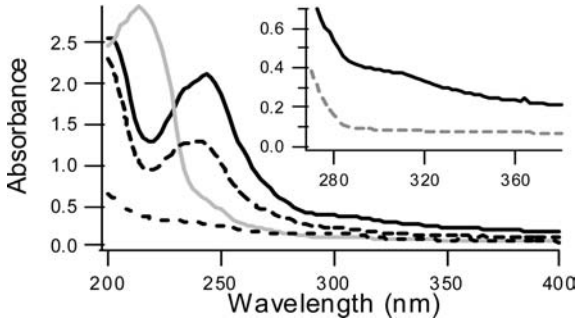

Figure 7. UV−visible absorption spectra of **1b**$^+$/Nafion immersed in water (black solid line), showing a progressive decrease in the absorption bands after 5 min of illumination (black dashed line) and free **1b**$^+$ in CH_2Cl_2 (gray solid line). Inset shows **1b**$^+$-Nafion immersed in water (black solid line) displaying Mn−O bands, and the free ligand $(MeOPh)_2PO_2H$ suspended in Nafion (gray dashed line). Extinction coefficients could not be calculated for Nafion membranes because accurate concentrations and path lengths were unknown.

Nafion environment clearly has a substantial effect on the UV absorption of **1b**$^+$ and the ligand.

Taking into account the red shift, the ligand bands, and the Mn−O bands (inset Figure 7) confirmed the presence of intact cubane within the Nafion membrane. Illumination of the **1b**$^+$/Nafion membrane immersed in water in the absence of an applied voltage resulted in a decline in intensity of the absorption over time (Figure 7 dashed). Without illumination in the presence of water, no significant decrease in intensity was observed over 24 h. Moreover, the UV−visible spectrum of **1b**$^+$ in Nafion remained unchanged upon exposure to light in the absence of water (unbiased **1b**$^+$/Nafion in air). This shows that the photoreaction requires water or a water environment to occur. The phosphinate ligand is sparingly soluble in water, so that if it is photodetached some fraction can diffuse out of the sampling region; this loss may account for the decrease of absorption due to the ligand band at 250 nm when there is no electrical bias to drive reformation of the cubium.

^{1}H NMR Spectra. Nafion membranes were cast onto the inside of NMR tubes, dried, and then doped with 2 mM solutions of **1b**$^+$ ClO_4^- or **1b**$^+$ $CH_3C_6H_4SO_3^-$ in CH_3CN. Tubes coated and doped in this way were rinsed with CH_3CN, dried at room temperature and then filled with D_2O. The ^{1}H NMR spectra are displayed in the Supporting Information, Figure S5. In all doped samples, ^{1}H NMR resonances were observed for the phenyl and methoxy protons of the phosphinate ligand, with a better signal-to-noise ratio observed for membranes doped with **1b**$^+$ $CH_3C_6H_4SO_3^-$. The multiplicity of phenyl protons in Nafion was typical of the splitting observed for the non-complexed, free ligand. The solution spectrum of the cubane-bound ligand in acetone displayed broad and weak proton signals due to the paramagnetism of the Mn core (Supporting Information, Figure S5). No resonances were observed for the *p*-toluenesulfonate counterion, confirming that anions are not taken up by the Nafion.

Since anions did not migrate into the Nafion, the negatively charged phosphinate ligands seen in the NMR spectra must be carried into the Nafion by the intact **1b**$^+$ complex. The data also reveal that, once present in the unbiased, aqueous Nafion, some portion

(45) Khangulov, S.; Sivaraja, M.; Barynin, V. V.; Dismukes, G. C. *Biochemistry* **1993**, *32*, 4912–4924.

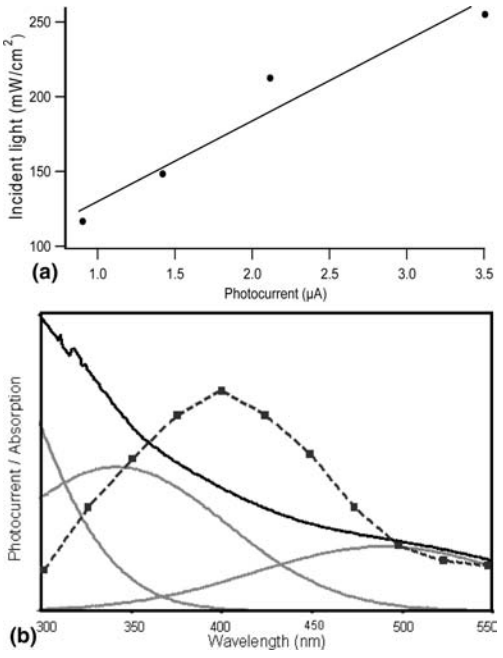

Figure 8. (a) Photocurrent of $\mathbf{1b}^+$/Nafion-glassy carbon electrode at 1.00 V vs Ag/AgCl, immersed in aqueous 0.1 M Na_2SO_4, measured with increasing incident light intensity. (b) Action spectrum of the photocurrent at 1.00 V (vs Ag/AgCl) generated by $\mathbf{1b}^+$-Nafion/glassy carbon (black dashed line), in 0.1 M Na_2SO_4, aq. (undoped, Nafion only baseline is subtracted) measured using a monochromated Xe lamp (see Supporting Information, Figure S6). Electronic absorption spectrum of $\mathbf{1b}^+$ in CH_2Cl_2 (black solid line) showing deconvoluted absorption bands (gray solid line).

of $\mathbf{1b}^+$ slowly reacts with water to release phosphinate ligand. This hydrolysis-induced ligand dissociation is not observed when the cubane is dissolved in the organic solution phase and must therefore be facilitated by the Nafion supporting environment and water. Since ligand detachment is an essential precursor to O_2 evolution in the gas phase photoreaction, we deduce that Nafion may assist in ligand detachment facilitating *catalytic* O_2-evolving photoreaction.

Photo-Action Spectrum. The size of the photocurrent generated by $\mathbf{1b}^+$-Nafion-coated glassy carbon at 1.00 V (vs Ag/AgCl) increased linearly with increasing light intensity, as shown for a representative electrode preparation in Figure 8a. A comparison of the UV−visible transmission spectrum of Nafion before and after doping with $\mathbf{1b}^+$ ClO_4^-, revealed that less than 1% of the illuminating light ($\lambda > 275$ nm, which is the cutoff for the glass electrochemical cell) was absorbed by the cubane. This highlights the exceedingly small amount of $\mathbf{1b}^+$ taken up by the Nafion and the fact that only a small amount of the total incident light is absorbed. Only a small fraction of the incident energy is therefore utilized.

We previously demonstrated[17a] that the size of the photocurrent was dependent on the wavelength of the illuminating light and that catalysis occurred using ultraviolet and visible light from 275 nm to beyond 500 nm. In the present work, the action spectrum of the photocurrent was measured using monochromated light and is shown in Figure 8b. Supporting Information, Figure S6 depicts the spectra of the different monochromated light bands used to measure the action spectrum, as well as the spectrum of the equivalent undoped Nafion-coated electrode. As mentioned above, the major absorption bands in the UV−visible spectrum of the cubium are red-shifted 30 nm in Nafion relative to the free cubium in open CH_2Cl_2 solution.[17a] The action spectrum has a peak at about 400 nm and a significant tail/shoulder extending to at least 550 nm (Figure 8b, dashed curve).

Because of the small quantity of $\mathbf{1b}^+$ in the Nafion, it was not possible to deconvolute the charge transfer region of the electronic spectrum. However, Gaussian deconvolution of the UV−visible-NIR spectrum of $\mathbf{1b}^+$ in CH_2Cl_2 solution indicated a band centered at 350 nm (Figure 8b). Given the observed red-shift of the phenyl ring absorption band of $\mathbf{1b}^+$ upon transfer from CH_2Cl_2 solution to Nafion, the maximum in the action spectrum found at 400 nm appears to match this charge transfer band. This band was previously assigned, using density functional theory (DFT) calculations, as having Mn-oxo charge transfer character, and is the photoactive band responsible for O_2 evolution in the gas phase.[44,28,29,46] The calculations suggest that light excitation into this band leads to an electron being promoted into an antibonding orbital on one Mn center, which promotes detachment of the corresponding bound phosphinate ligand. In Nafion, the action spectrum extends further to the red beyond this band where there is a weak shoulder (Figure 8b). This region includes a group of 3d ligand-field transitions on Mn, which suggests that activation of this class of transitions may assist in photocurrent generation.

Influence of the Nafion Itself. Nafion does more than just provide an interface for the cubane and water molecules to interact. As previously reported light activation of the cubium in the gas phase results in O_2 evolution; however, this process is not observed on irradiation of solutions. The interaction between Nafion and the phosphinate ligands, as revealed by both NMR and UV−vis spectral data, suggests that it may increase the flexibility of the Mn_4O_4 core by weakening the ligand binding. The sulfonic acid groups in the Nafion framework (acid $pK_a \sim -5$) may also protonate labile phosphinate ligands ($pK_a \sim 2$) thereby slowing the rebinding of free ligands during the O_2 formation. Thus, the interaction of the sulfonic acid/sulfonate groups with the cubium/phosphinate ligands appears to assist the light induced ligand disruption required to facilitate O_2 evolution.

As noted in our communication,[17a] proton generation in the aqueous solution displays an initial lag relative to the observed photocurrent, suggesting that the Nafion acts as a proton "buffer" or "sink". This feature may be essential to the removal of protons from water during the catalytic oxidation process. Indeed, it appears that the hydrophobic and hydrophilic domains, and the proton exchange sites of the Nafion, create an environment about the cubane that facilitates proton conduction during the catalytic process.

Reactive intermediates appear to be held within the catalytic site by a combination of hydrophilic, hydrophobic, and electrostatic forces that facilitate the interaction between the reactants and catalyst. This may be prolonging the lifetime of these intermediates, increasing

(46) Carrell, T. G.; Cohen, S.; Dismukes, G. C. *J. Mol. Catal. A: Chem.* **2002**, *187*, 3–15.

their opportunity to react while products are readily transported away from the reaction site.

Combined Effects of Light, Electrochemical Biasing, and the Nafion Interface. From the aforementioned photochemistry, the observation of the intact cubium prior to illumination and the formation of the $Mn^{III}Mn^{IV}$ species in the presence of applied potential, several mechanisms can be postulated. One possibility is shown in Scheme 1. Application of a potential to the cubium doped Nafion regenerates $\mathbf{1b}^+$ or a cubium-like species, which continues to undergo a very slow reaction in the dark in the presence of water. Light excitation of the cluster causes a dramatic increase in the reaction with water. The exact mechanism and indeed the reactive species remain unclear, but the spectral data collected suggests the following as one possibility: Irradiation of the oxidized manganese cluster excites a charge transfer transition which has previously been shown to induce the release of one bridging phosphinate ligand from the manganese-oxo core in the gas phase. In the gas phase, this allows flexing of the cubane framework enabling two bridging *O* atoms on the open face of the cubane to form a peroxo intermediate, a process aided by a two-electron intramolecular reduction of the two Mn atoms on the lower face.[23,30] Dioxygen is then formed by a further two-electron intramolecular reaction and ultimately released, leaving the previously described *open butterfly* complex, $[Mn_4O_2L_5]^{2+}$. In the Nafion system, an analogous pathway, involving Mn-species whose coordination sphere is completed by water molecules, is supported by the observation of free ligand and a species containing a spin-coupled Mn^{III}-$(\mu$-O$)_x$-Mn^{IV} subcluster (Mn dimer or tetramer as yet unclear). These products were not observed following irradiation of cubium in solution suggesting that the Nafion environment plays a crucial role in facilitating the observed photoreaction.

The detection of the cubium or a cubium like Mn_4-oxo cluster in the Nafion as the dominant species before and after catalytic cycling suggests that, following ligand release and oxygen evolution, the resulting cluster interacts with water molecules within the Nafion and is oxidized by the applied potential to a reactive Mn_4-oxo complex to complete the cycle. This process is accompanied by the release of protons. One possibility for cluster reformation following O_2 evolution is a two-electron oxidation of a reduced butterfly like core $[L_5Mn_4O_2]^{2+}$, to form species such as $[L_5Mn_4O_3]^{2+}$ (Scheme 1). Such a species is a potential candidate for the 16-line EPR signal, as described above. Two-electron oxidation of the postulated intermediate reforms the catalytically active tetramanganese cluster. In support of the proposed two-electron redox steps in this cycle, the cubanes are known to readily undertake two-electron redox reactions.[32,46] It is unclear whether the resulting Mn_4-oxo cluster rebinds free phosphinate ligands or is supported by the sulfonate groups of Nafion.

Drawing mechanistic conclusions about water-oxidizing catalysts is extremely difficult. This is highlighted by the fact that after 25 years of research on the Ru dimer, $[\{(bipy)_2(H_2O)Ru^{III}\}(\mu\text{-O})]^{4+}$ (bipy = 2,2′-bipyridine), the mechanism of this action is still being debated.[47−49] Using the mechanistic hypotheses proposed above as a guide, we are undertaking detailed spectral studies aimed at resolving further details of the catalytic cycle. These studies will take into account recent kinetic data which indicate that the mechanism of substitution of bridging oxo-groups in cubium $\mathbf{1}^+$ and $[((tpy)(H_2O)Mn)_2(\mu\text{-O})_2]^{3+}$ is, in fact, associative and that reactions at these Mn centers are likely to proceed via a transition state of increased coordination number.[50]

Turnover Frequency. The quantity of catalyst present in the Nafion membrane and in electrical contact with the electrode was estimated by bulk electrolysis using the observed $\mathbf{1b/1b}^+$ process. This technique assumes that all of the collected electrons arise from the electrochemical reduction of $\mathbf{1b}^+$. As such, it provides the best estimate of the number of $\mathbf{1b}^+$ cations present within the Nafion that are in electrical contact with the electrode. It does not indicate the total quantity of $\mathbf{1b}^+$ in the Nafion since it excludes material not in electrical contact.

The maximum turnover frequency was calculated using the peak photocurrent (see example in Figure 2) measured immediately after exposure of the $\mathbf{1b}^+$-Nafion-coated electrode to illumination at 150 mW/cm^2 and at 1.00 V (vs Ag/AgCl).[17a] Under these conditions, a peak photocurrent of 7.95 μA was recorded for a $\mathbf{1b}^+$-Nafion-coated glassy carbon electrode of 3 mm diameter. Bulk electrolysis indicated that there were 0.53 μg of electroactive species present, which equates to a peak turnover frequency of 270 O_2 molecules h^{-1} per electroactive catalyst molecule, based on the production of one O_2 molecule requiring 4 e^-.[17a] Over a range of membrane preparations the peak turnover frequencies fell within the range 100−270 molecules O_2 h^{-1} catalyst^{-1}. After extended illumination for 10 h, the turnover rate, based on observed photocurrents, was about 50 molecules O_2 h^{-1}. A different membrane studied in our previous work had a turnover rate of about 20 molecules O_2 h^{-1} after 65 h of operation. Integration over this period reveals that turnover numbers (TON) greater than 1000 O_2 molecules catalyst^{-1} were achieved without complete decomposition of the catalyst.[17a] This TON compares favorably with those of the previously described catalysts summarized in Table 1 and exceed the values reported previously for first row transition metal catalysts. By comparison, the natural *PSII-WOC* system achieves turnover rates in vivo ranging from about 500 s^{-1} to zero, which can be limited by either electron transport or proton transport, depending upon species and conditions.[51]

Conclusions

The biologically inspired $[Mn_4O_4]^{7+}$ cubane core supported by phosphinate ligands has been shown to be a highly effective catalyst for the oxidation of water molecules to molecular oxygen when suspended in a Nafion membrane.

(47) Binstead, R. A.; Chronister, C. W.; Ni, J.; Hartshorn, C. M.; Meyer, T. J. *J. Am. Chem. Soc.* **2000**, *122*, 8464–8473.

(48) Yamada, H.; Siems, W. F.; Koike, T.; Hurst, J. K. *J. Am. Chem. Soc.* **2004**, *126*, 9786–9795.

(49) Cady, C. W.; Crabtree, R. H.; Brudvig, G. W. *Coord. Chem. Rev.* **2008**, *252*, 444–455.

(50) Ohlin, C. A.; Brimblecombe, R.; Spiccia, L.; Casey, W. H., *Dalton Trans.* **2009**, DOI: 10.1039/b906169.

(51) Ananyev, G. M.; Dismukes, G. C. *Photosynth. Res.* **2005**, *84*, 355–365.

It does so using both light and electrical energy at a low overpotential (0.38 V vs NHE). In this system, Nafion provides an oxidatively inert support and hydrophobic environment that red-shifts the electronic absorptions of the cluster, while allowing it to interact with water molecules and providing proton conduction sites essential for continuous turnover. In this study, the cubium $\mathbf{1b}^{+}$ is proposed to be the dominant species that is regenerated upon electrooxidation within the Nafion membrane during catalytic turnover and is minimally a precursor to the O_2-evolving species. Spectroscopic evidence reveals that the cubium when doped in Nafion reacts with water and (partially) dissociates a phosphinate ligand. Catalysis occurs by a two-step process involving an initial light driven step, where the highly oxidized tetra-manganese cluster is activated for oxygen release, and a second electrically driven step where, in the presence of water, the highly oxidized catalytic species is reformed and protons are released.

Further investigations are being undertaken to resolve specific details of the catalytic cycle and possible intermediate species. Toward improving the current density of the system, we are focusing on increasing the concentration of electroactive species within the Nafion and improving the interfacial charge transfer within the membrane.

Acknowledgment. G.C.D. acknowledges the NIH for grant support (GM-39932) and a Lemberg Travel Award. L.S., G.S., and A.M.B. acknowledge the support of the Australian Research Council. R.B. acknowledges the support of an Australian Postgraduate Award, a Monash University Postgraduate Publication Award, and a Fulbright Postgraduate Award. G.S. thanks the Australian Academy of Sciences for a Travel Fellowship. The authors thank G. Felton, M. Rotstein, and J. Sheats for support in catalyst development and M. Belousoff, N. Fay, I. Pelczer, and G. Ananyev, for assistance with data preparation, photoelectrochemistry, NMR spectroscopy, and instrumentation, respectively.

Supporting Information Available: ^{1}H NMR spectra in solution and in Nafion, photoaction spectra of individual components, electronic absorption spectrum in Nafion, cyclic voltammograms in Nafion and an SEM image of a sliced edge of the Nafion coating are provided.[26] This material is available free of charge via the Internet at http://pubs.acs.org.